3-Bromopyruvate alleviates the development of monocrotaline-induced rat pulmonary arterial hypertension by decreasing aerobic glycolysis, inducing apoptosis, and suppressing inflammation

Jie Liu[1], Wang Wang[2,3], Lei Wang[3,4], Xian-Mei Qi[2,3], Yu-Hui Sha[2,3], Ting Yang[3,4]

[1]Department of Immunology, Capital Medical University, Beijing 100069, China;
[2]Department of Physiology and Pathophysiology, Capital Medical University, Beijing 100069, China;
[3]Beijing Key Laboratory of Respiratory and Pulmonary Circulation Disorders, Capital Medical University, Beijing 100069, China;
[4]Department of Respiratory and Critical Care Medicine, China-Japan Friendship Hospital, Beijing 100029, China.

Abstract

Background: Pulmonary arterial hypertension (PH) is a progressive disease with limited therapeutic options, ultimately leading to right heart failure and death. Recent findings indicate the role of the Warburg effect (aerobic glycolysis) in the development of PH. However, the effect of the glycolysis inhibitor 3-bromopyruvate (3-BrPA) on the pathogenesis of PH has not been well investigated. This study aimed to determine whether 3-BrPA inhibits PH and its possible mechanism.

Methods: PH was induced in adult Sprague-Dawley rats by a single intraperitoneal injection of monocrotaline (MCT). 3-BrPA, or phosphate-buffered saline (PBS) was administered via intraperitoneal injection every other day from the first day of MCT-injection to 4 weeks of follow-up, and indices such as right ventricular systolic pressure (RVSP), right ventricular hypertrophy index (RVHI), pulmonary arteriolar remodeling indicated by percent media thickness (% MT), lactate levels and glucose consumption, were evaluated. Pulmonary arteriolar remodeling and right ventricular hypertrophy were observed in hematoxylin-eosin-stained lung sections. Western blotting, immunohistochemistry, and/or immunofluorescence analyses were used to measure the expression of relevant proteins. A cytochrome C release apoptosis assay and terminal deoxynucleotidyl transferase-mediated dUTP-biotin nick end-labeling staining were used to measure cell apoptosis.

Results: MCT-induced PH showed a significant increase in glucose consumption (0 *vs.* 4 weeks: 0.87 ± 0.23 *vs.* 2.94 ± 0.47, $P = 0.0042$) and lactate production (0 *vs.* 4 weeks: 4.19 ± 0.34 *vs.* 8.06 ± 0.67, $P = 0.0004$). Treatment with 3-BrPA resulted in a concomitant reduction in glucose consumption (1.10 ± 0.35 *vs.* 3.25 ± 0.47, $P = 0.0063$), lactate production (5.09 ± 0.55 *vs.* 8.06 ± 0.67, $P = 0.0065$), MCT-induced increase in RVSP (39.70 ± 2.94 *vs.* 58.85 ± 2.32, $P = 0.0004$), pulmonary vascular remodeling (% MT, $43.45\% \pm 1.41\%$ *vs.* $63.66\% \pm 1.78\%$, $P < 0.0001$), and right ventricular hypertrophy (RVHI, $38.57\% \pm 2.69\%$ *vs.* $62.61\% \pm 1.57\%$, $P < 0.0001$) when compared with those of the PBS-treated group. 3-BrPA, a hexokinase 2 inhibitor, exerted its beneficial effect on PH by decreasing aerobic glycolysis and was also associated with inhibiting the expression of glucose transporter protein-1, inducing apoptosis, and suppressing inflammation.

Conclusions: 3-BrPA might have a potential beneficial effect on the PH treatment.

Keywords: Pulmonary arterial hypertension; Monocrotaline; 3-Bromopyruvate; Aerobic glycolysis

Introduction

Pulmonary arterial hypertension (PH) is a progressive and life-threatening disease characterized by pulmonary vasoconstriction and remodeling, ultimately leading to right heart failure and death. Clinically, limited treatments mainly focus on vasodilatation to alleviate symptoms and improve quality of life.[1] More recent advances are based on targeting pulmonary vascular remodeling to mainly reduce the abnormal proliferation of pulmonary arterial cells. However, PH remains relatively incurable, and its prognosis remains unfavorable.[2] Mounting evidence, including that of our lab, indicates that dysregulation of metabolic pathways plays an important role in fundamental and early components of PH.[3,4]

One of the metabolic pathways is named the Warburg effect, also known as aerobic glycolysis, and converts

Access this article online

Quick Response Code:

Website: www.cmj.org

DOI: 10.1097/CM9.0000000000000577

Jie Liu and Wang Wang contributed equally to this work.

Correspondence to: Dr. Ting Yang, Department of Respiratory and Critical Care Medicine, China-Japan Friendship Hospital, Beijing 100029, China
E-Mail: dryangting@qq.com

Chinese Medical Journal 2020;133(1)

Received: 14-07-2019 **Edited by:** Qiang Shi

pyruvate to lactate acid despite the presence of abundant oxygen.[5] The Warburg effect serves as a critical mechanism in the development of PH by largely driving cellular hyperproliferation and apoptosis resistance.[6] Recent studies have shown that the glycolysis inhibitor 3-bromopyruvic acid (3-BrPA) is a promising anti-cancer compound capable of inducing rapid cell death in numerous cancer cells with limited cytotoxic effects against normal cells by inhibiting the activities of metabolic enzymes such as glyceraldehyde-3-phosphate dehydrogenase (GAPDH), hexokinase 2 (HK-2), succinic dehydrogenase.[7-9] In addition, 3-BrPA is able to dissociate and inhibit mitochondria-bound HK-2 function, thereby allowing proapoptotic molecules to promote the release of Cyto C into the cytosol and induce caspase-3 (Casp 3) activation.[10] It has been reported that 3-BrPA could reverse hypoxia-induced PH by inhibiting glycolysis,[11] but until now, the effect of 3-BrPA on the development of monocrotaline (MCT)-induced PH has not been well studied.

In the present study, we hypothesized that treatment with 3-BrPA may be effective in the MCT-induced PH rat model. Therefore, this study was designed to evaluate the level of aerobic glycolysis and the effect of 3-BrPA in MCT-induced PH and to explore the mechanisms of the potential beneficial effect of 3-BrPA on PH treatment, with the aim of finding a novel strategy for PH treatment.

Methods

Animals

Adult male Sprague-Dawley rats weighing 250 to 300 g were purchased from the Vital River Laboratory Animal Technology Company of Beijing in China and maintained in a temperature-controlled room with a 12-12 h light-dark cycle. All animal care and experiments were approved by the Institutional Animal Care and Use Committee of Capital Medical University and performed in accordance with the Management of Laboratory Animals published by the Ministry of Science and Technology of the People's Republic of China.

The PH model was induced by a single intraperitoneal injection (60 mg/kg, i.p.) of MCT (Catalog No. C2401; Sigma-Aldrich, Saint Louis, USA). Control animals were given a single intraperitoneal injection of the same volume of 0.9% NaCl. For the 3-BrPA (Catalog No. 16490; Sigma-Aldrich) treatment, MCT-induced PH rats were injected intraperitoneally with either 3-BrPA (2 mmol/L, i.p.)[12] or the same volume of phosphate-buffered saline (PBS) every other day beginning on the day of MCT injection to 4 weeks of follow-up.

Measurement of the right ventricular systolic pressure

The rats were anesthetized with 2% sodium pentobarbital (45 mg/kg, i.p.). A catheter filled with heparinized saline was inserted into the right ventricle (RV) via the jugular vein to measure right ventricular systolic pressure (RVSP). The RVSP was then recorded by a PowerLab data acquisition system (AD Instruments, Sydney, Australia) and digitized by LabChart software (AD Instruments). The average RV pressure was measured during systole to determine the individual RVSP.

Measurements of glucose and lactate concentration

Before the experiments and after hemodynamic measurement, the serum of the rats was collected. Then, the rats were euthanized by exsanguination. The glucose and lactate levels were detected using a lactate- and glucose-measuring instrument (EKF Diagnostics, Barleben, Germany). Glucose levels were detected at 0 and 4 weeks, and glucose consumption = (glucose level at 0 week) − (glucose level at 4 weeks).

Measurement of right ventricular hypertrophy

Heart tissue was removed. The RV free wall was dissected from the left ventricle (LV) and ventricular septum (S). The RV hypertrophy index (RVHI) was calculated by the wet weight ratio of the RV to the LV plus S using the formula: RV/(LV + S) × 100%. The ratio of RV weight to body weight (BW) was also examined.

Cardiomyocyte cross-sectional diameter was determined in the RV and LV as measures of cardiac ventricular tissue remodeling. Four-micron sections of the RV and LV were stained with hematoxylin and eosin (H&E), and the diameter of individual cardiomyocytes in histological sections of the left and right ventricular walls was measured. Microscopic images were analyzed in a blinded manner using a Nikon microscope digital camera system and its image analysis program (Nikon, Tokyo, Japan).

Lung tissue preparation and morphometric analysis

The left lungs embedded in paraffin were serially sectioned at a thickness of 4-μm for standard H&E staining, immunohistochemistry, and immunofluorescence. Pulmonary vessels with external diameters smaller than 150 μm were selected. Medial thickness was determined as follows: percent medial thickness (% MT) = ($\text{circumference}_{ext}/\pi$ − $\text{circumference}_{int}/\pi$)/($\text{circumference}_{ext}/\pi$) × 100%. The $\text{circumference}_{ext}$ and $\text{circumference}_{int}$ were demarcated by the external and internal elastic lamina, respectively. Images of pulmonary vessels were captured with a Nikon microscope digital camera system, and circumferences were measured with the image analysis program.

Immunohistochemical analysis

Immunoreactivity of HK-2 was detected in paraffin-embedded human lung sections using a rabbit anti-human HK-2 antibody (1:500 dilution, Catalog No. ab209847, Abcam, UK). Positive signals were visualized using an horseradish peroxidase-conjugated goat anti-rabbit secondary antibody (1:200 dilution, Catalog No. 8114, CST, Danvers, MA, USA). The positive cells were developed by diaminobenzidine (DAB) reagent, and the nuclei were stained with hematoxylin.

Assessment of macrophage infiltration

Staining for CD68 (Sigma-Aldrich) by using standard immunofluorescence protocols was performed to quantify

the degree of macrophage lung infiltration. Briefly, CD68 expression levels were detected in paraffin-embedded lung sections using the anti-CD68 antibody (1:200 dilution, Catalog No. HPA048982; Sigma-Aldrich), and protein expression was visualized using Alex Fluor 594 goat anti-rabbit secondary antibodies (1:200 dilution, Catalog No. ZF-0516; ZSGB-BIO, China). Nuclei were counterstained with 4′,6-diamidino-2-phenylindole.

Western blotting analysis

For the Western blotting analysis, 80 μg of protein samples were separated on the sample buffer by sodium dodecyl sulfate-polyacrylamide gel electrophoresis, proteins were then transferred to nitrocellulose membranes. Membranes were blocked at room temperature for 1 h in 5% non-fat dry milk in PBS, followed by incubation with anti-HK2 (1:100 dilution), anti-Cyto C (1:50 dilution, Catalog No. ab13575; Abcam), anti-voltage dependent anion channel (VDAC) (1:1000 dilution, Catalog No. ab15895; Abcam), anti-cleaved Casp 3 (1:50 dilution, Catalog No. ab2302; Abcam), and anti-β-actin (1:6000 dilution, Catalog No. a0516; Sigma-Aldrich) or anti-GAPDH (1:6000 dilution, Catalog No. G9454; Sigma-Aldrich) antibodies overnight at 4°C. After incubated with secondary antibodies, the protein bands were visualized using the LI-COR Odyssey infrared double-fluorescence imaging system (LI-COR Biosciences, Lincoln, Nebraska, USA). The relative density value of each target protein band was normalized to the density of the corresponding β-actin, VDAC, or GAPDH band.

TUNEL staining

The terminal deoxynucleotidyl transferase-mediated dUTP-biotin nick end labeling (TUNEL) assay was performed with *in situ* cell death detection kits (Catalog No. C1091; Beyotime Biotechnology, Beijing, China) according to the manufacturer's instructions. Briefly, the slides were rinsed twice with PBS. The samples were treated with proteinase K solution for 30 min at 37°C. The slides were rinsed twice with PBS. The area around each sample was dried, and 50 μL TUNEL reaction mixture was added to the sample and incubated for 60 min at 37°C in a humidified atmosphere in the dark. The slides were rinsed three times with PBS, 50 μL converter-peroxidase was added to the samples and incubated for 30 min at 37°C in a humidified atmosphere in the dark. The slides were rinsed three times with PBS, the positive cells were detected by diaminobenzidine reagent, and the nuclei were stained with hematoxylin.

Cytochrome c release apoptosis assay

For the rapid, sensitive and accurate detection of cytochrome c translocation from mitochondria into the cytosol during apoptosis in tissues, cell apoptosis was determined using a Cyto C release apoptosis assay kit (Catalog No. ab65311; Abcam) according to the manufacturer's instructions.

Statistical analysis

Data are expressed as the mean ± standard error. Unpaired Student's *t* test was used for comparisons between two groups. One-way analysis of variance with the Newman-Keuls test was used to evaluate differences between more than two groups. A value of $P < 0.05$ was considered statistically significant.

Results

Metabolic characteristics of MCT-induced PH rats

Four weeks after MCT injection, increases in RVSP [Figure 1A] (25.47 ± 1.27 *vs.* 52.32 ± 3.72 mmHg, 1 mmHg = 0.133 kPa), RVHI [Figure 1B] (28.16 ± 0.89 *vs.* $55.39 \pm 4.06\%$), and pulmonary vascular remodeling [Figure 1C] (% MT: $22.83\% \pm 0.75\%$ *vs.* $61.20\% \pm 1.79\%$) were observed. The lactate and glucose levels of MCT rats were detected in serum at 2 and 4 weeks after MCT injection. Compared with the baseline concentration, the concentration of lactate was upregulated in the serum of MCT rats and significantly increased at 4 weeks after MCT injection ($P < 0.001$) [Figure 1D]. In addition, glucose consumption was significantly higher in MCT rats compared with that of the control group ($P < 0.01$) [Figure 1E]. These results indicate that MCT-induced PH increased the rate of aerobic glycolysis.

Effects of 3-BrPA on glycolysis

The typical features of aerobic glycolysis are increased glucose consumption and lactate production. To understand the effects of 3-BrPA on glycolysis in MCT-induced PH, rats were injected with MCT and received injections of PBS or 3-BrPA every other day for 4 weeks. Our data showed that 3-BrPA treatment significantly decreased the concentration of lactate ($P < 0.01$) compared to that in the PBS-treated rats [Figure 2A]. Rats treated with 3-BrPA showed significantly lower ($P < 0.01$) glucose consumption than that of PBS-treated rats [Figure 2B]. These results suggest that 3-BrPA inhibits glycolysis in PH.

Effects of 3-BrPA on BW and right ventricular systolic pressure

Figure 2C depicts the BWs, demonstrating that all rats had increased BW at 4 weeks after MCT injection ($P < 0.001$). In PBS-treated MCT rats, BW was reduced by $17.51\% \pm 0.54\%$ ($P < 0.001$); in the 3-BrPA-treated group, BW was reduced by $21.39\% \pm 1.72\%$ ($P < 0.001$) at 4 weeks after MCT injection compared with that of the control group.

RVSP is used as an indicator of pulmonary arterial systolic pressure. MCT injection led to PH characterized by a significant increase in RVSP to 58.85 ± 2.32 mmHg 4 weeks after MCT injection compared with that of the control group (26.38 ± 0.67 mmHg) ($P < 0.001$). Treatment with 3-BrPA significantly reduced the MCT-induced increase in RVSP to 39.70 ± 2.94 mmHg compared with that of the PBS-treated MCT rats ($P < 0.001$) [Figure 2D]. Taken together, these results show that MCT injection effectively induces PH in rats and is distinctly attenuated by 3-BrPA.

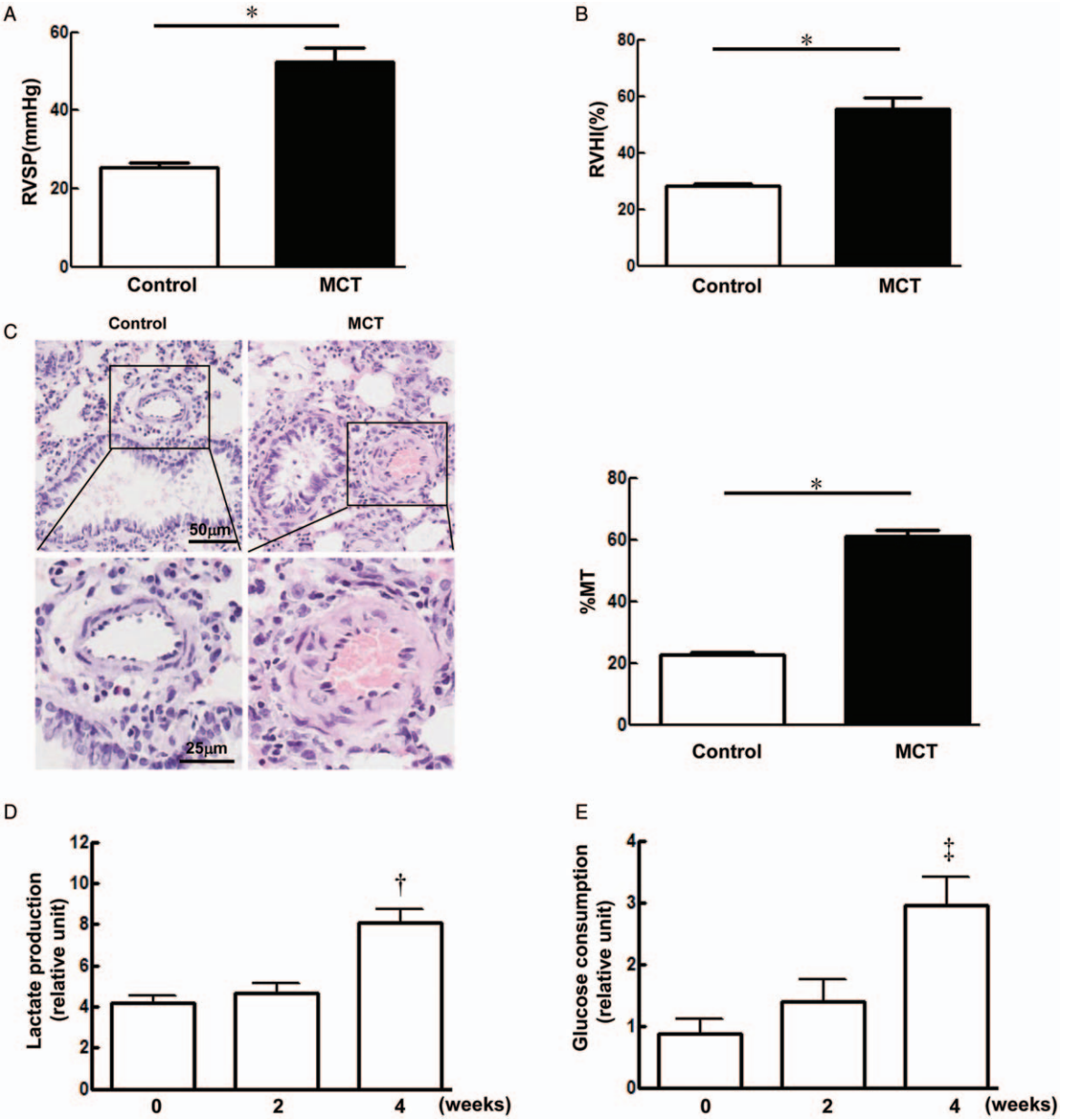

Figure 1: Metabolic characterization of MCT rats. (A) RVSP and (B) RVHI in rat PH models of MCT compared with those in the control ($n = 8$ in each group). $^{*}P < 0.001$ *vs.* control. (C) Hematoxylin-eosin staining and % MT of pulmonary arterioles. $^{*}P < 0.001$ *vs.* control. (D) Lactate production ($^{\dagger}P < 0.001$ *vs.* 0 week, $n = 5$ in each group) and (E) glucose consumption ($^{\ddagger}P < 0.01$ *vs.* 0 week, $n = 6$ in each group) of MCT rats were detected in serum at 2 or 4 weeks after MCT injection. 1 mmHg = 0.133 kPa. % MT: Percent medial thicknesses; MCT: Monocrotaline; RVHI; Right ventricular hypertrophy index; RVSP: Right ventricular systolic pressure.

Effects of 3-BrPA on pulmonary arteriolar remodeling

Progressive medial thickening is a major characteristic in PH. To investigate the effects of 3-BrPA on MCT-induced remodeling of pulmonary arterioles, H&E staining of lungs from control, PBS-treated and 3-BrPA-treated MCT rats was used for morphometric analysis. Representative specimens showed that the medial thickness of peripheral pulmonary vessels was evidently increased in PBS-treated MCT rats. However, these changes appeared to be ameliorated in 3-BrPA-treated MCT rats [Figure 2E].

Quantitative analysis of %MT is used to evaluate the medial thickening of pulmonary arterioles. As shown in Figure 2F, the %MT of peripheral pulmonary vessels showed enhanced medial wall thickness from $26.39\% \pm 1.17\%$ in the control group to $63.66\% \pm 1.78\%$ in the PBS-treated group in intra-acinar vessels sized smaller than 150 μm ($P < 0.001$). In the 3-BrPA-treated group, the increase in medial wall thickness was significantly decreased to $43.45\% \pm 1.41\%$ compared with that of the PBS-treated MCT rats ($P < 0.001$). These results demonstrate the anti-remodeling impact of 3-BrPA on the pulmonary vasculature.

Effects of 3-BrPA on right ventricular hypertrophy

The presence of right ventricular hypertrophy is a hallmark of end-stage PH. The ratios of RV/BW and RVHI express the degree of RV hypertrophy. Compared to the ratio in

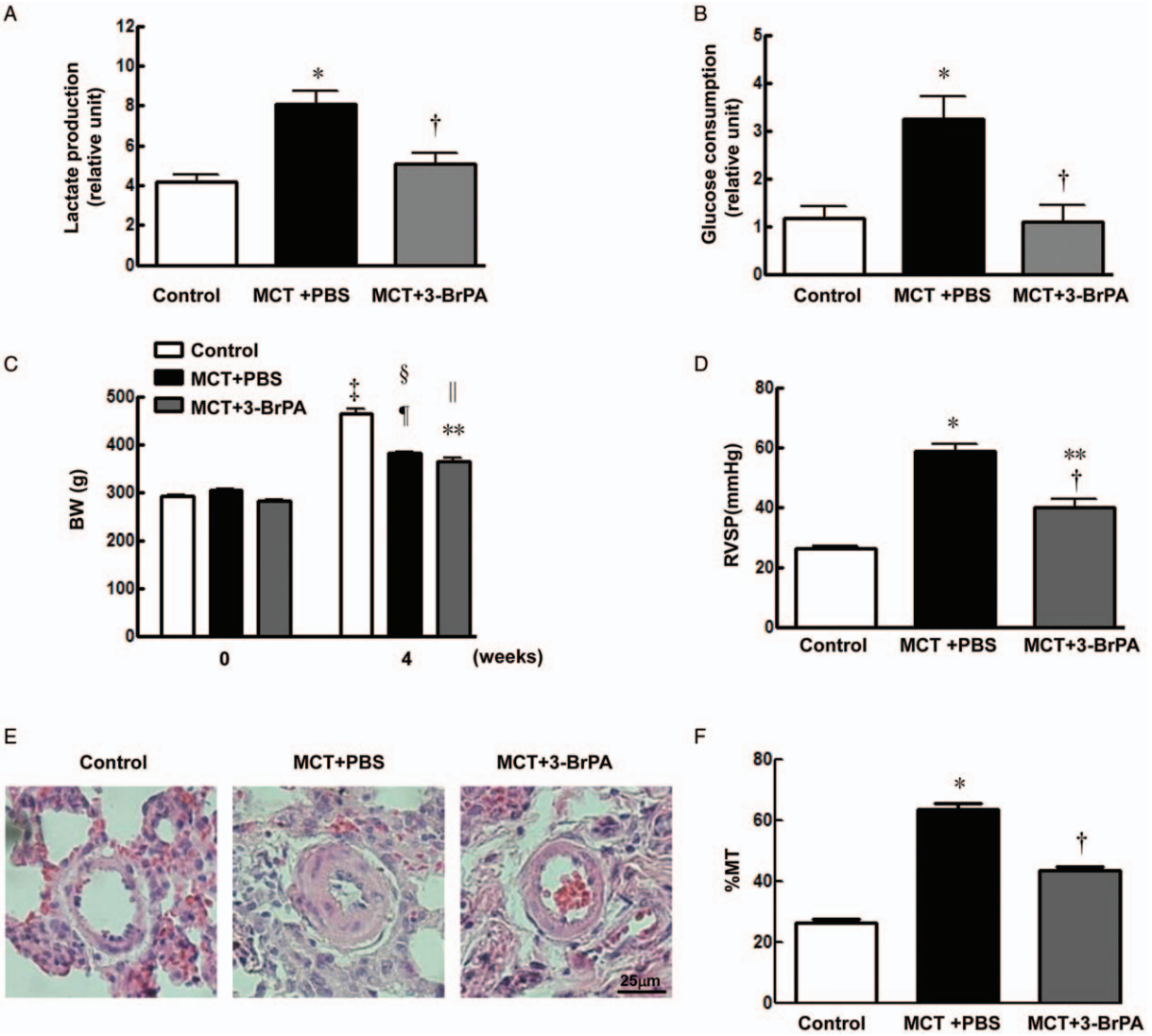

Figure 2: Effects of 3-BrPA on MCT rats. (A) Lactate production ($^{*}P < 0.001$ *vs.* control; $^{\dagger}P < 0.01$ *vs.* MCT + PBS, $n = 6$ in each group) and (B) glucose consumption ($^{*}P < 0.01$ *vs.* control; $^{\dagger}P < 0.01$ *vs.* MCT + PBS, $n = 5$ in each group) were detected in control, MCT + PBS-treated, and MCT + 3-BrPA-treated rats. (C) BW ($^{\ddagger,\S,\|}P < 0.001$ *vs.* 0 week; $^{\P,**}P < 0.001$ *vs.* control, $n = 6$ in each group) and (D) RVSP ($^{*,**}P < 0.001$ *vs.* control; $^{\dagger}P < 0.001$ *vs.* MCT + PBS, $n = 6$ in each group) were determined in control, MCT + PBS-treated, and MCT + 3-BrPA-treated rats. (E) Representative hematoxylin-eosin staining in rats from control (left), MCT + PBS (middle), and MCT + 3-BrPA (right) groups. Scale bar = 25 μm. (F) Quantification of the percent medial thickness of pulmonary arterioles sized <150 μm in diameter ($^{*}P < 0.001$ *vs.* control; $^{\dagger}P < 0.001$ *vs.* MCT + PBS, $n = 6$ in each group). 1 mmHg = 0.133 kPa. 3-BrPA: 3-Bromopyruvate; BW: Body weight; MCT: Monocrotaline; % MT: Percent medial thicknesses; PBS: Phosphate-buffered saline.

the control group, the RV/BW ratio increased significantly by 1.13 ± 0.18 fold ($P < 0.001$) in PBS-treated MCT rats at 4 weeks. 3-BrPA treatment reduced the RV/BW ratio by 29.90% ± 6.03% ($P < 0.01$) at 4 weeks after MCT injection [Figure 3A]. RVHI in PBS-treated MCT rats also demonstrated a marked elevation of 62.61% ± 1.57%, compared with that of the control group (28.25% ± 0.48%) ($P < 0.001$) [Figure 3B]. A prominent reduction in RVHI was observed in rats treated with 3-BrPA (38.57% ± 2.69%) compared with that of the PBS-treated MCT rats ($P < 0.001$).

Ventricular hypertrophy was also evaluated by measuring the diameters of cardiomyocytes. Figure 3C depicted representative H&E staining of heart tissue for control PBS-treated and 3-BrPA-treated MCT-Rats of heart tissues. The diameters of cardiomyocytes were further measured as a parameter of ventricular hypertrophy. Cardiomyocyte diameter was enhanced from 21.83 ± 0.21 to 40.07 ± 0.49 μm with PBS treatment and significantly reduced to 29.26 ± 0.40 μm with 3-BrPA treatment in MCT rats [Figure 3D]. The cardiomyocyte diameter remained largely unchanged in the LV [Figure 3E]. These data demonstrate that 3-BrPA can effectively protect against the MCT-triggered hypertrophy of individual cardiomyocytes in the RV.

Effects of 3-BrPA on the expression of HK-2 and glucose transporter protein-1 in MCT-induced PH rats

HK-2 is the key mediator of glucose metabolism and catalyzes the first rate-limiting step during aerobic glycolysis. Therefore, the expression of HK-2 in the lungs of MCT rats was observed by Western blotting

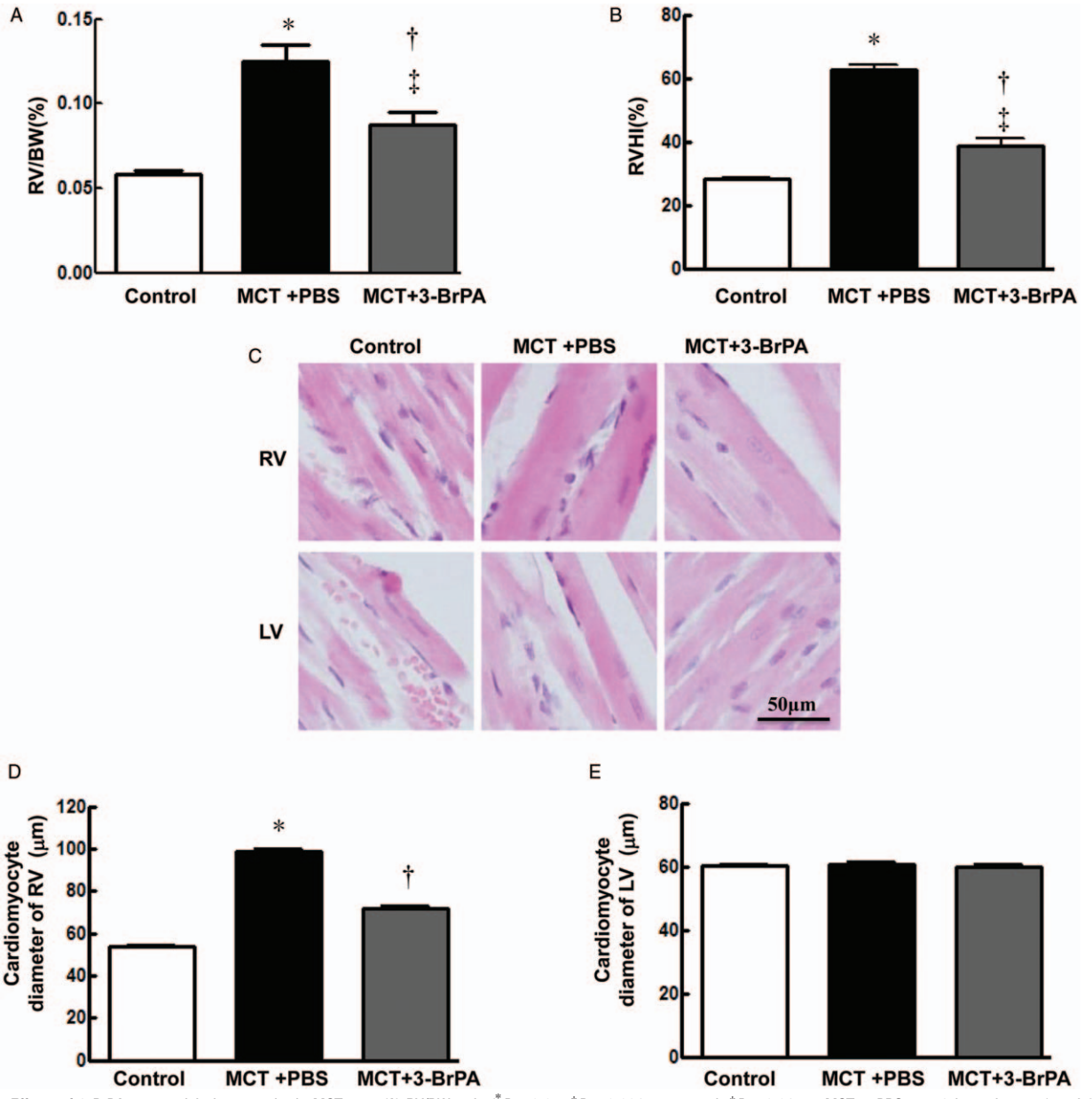

Figure 3: Effects of 3-BrPA on ventricle hypertrophy in MCT rats. (A) RV/BW ratio ($^{*}P < 0.05$, $^{\dagger}P < 0.001$ *vs.* control; $^{\ddagger}P < 0.01$ *vs.* MCT + PBS, $n = 6$ in each group) and (B) RVHI ($^{*,\dagger}P < 0.001$ *vs.* control; $^{\ddagger}P < 0.01$ *vs.* MCT + PBS, $n = 6$ in each group) were determined in control, MCT + PBS-treated, and MCT + 3-BrPA-treated groups. (C) Representative hematoxylin-eosin staining of the right ventricle (upper panel) and the left ventricle (lower panel) derived from control (left), MCT + PBS (middle), and MCT + 3-BrPA (right) groups. Scale bar = 50 μm. (D) Cardiomyocyte diameter in the right ventricle in each group ($^{*}P < 0.001$ *vs.* control; $^{\dagger}P < 0.001$ *vs.* MCT + PBS, $n = 5$ in each group). (E) Cardiomyocyte diameter of the left ventricle in each group ($n = 5$ in each group). 3-BrPA: 3-Bromopyruvate; BW: Body weight; LV: Left ventricle; MCT: Monocrotaline; PBS: Phosphate-buffered saline; RV: Right ventricle; RVHI: Right ventricular hypertrophy index.

analysis at 2 and 4 weeks after MCT injection. Compared with the baseline expression, the expression of HK-2 was upregulated in the lungs of MCT rats and significantly increased at 4 weeks after MCT injection ($P < 0.05$) [Figure 4A]. These results suggest that MCT-induced PH is associated with HK-2 upregulation. It has been reported that 3-BrPA is an inhibitor of HK-2, and the effects of 3-BrPA on the expression of HK-2 in MCT-induced PH rats were examined by Western blotting and immunohistochemical analysis. The results showed that after 3-BrPA injection in MCT rats, the expression of HK-2 in rat lungs was downregulated compared to that of PBS-treated MCT rats [Figure 4B and 4C]. The results of the immunohistochemical analysis showed that HK-2 stained mainly in the perivascular area, and then we investigated the localization of HK-2 by co-staining HK-2 and smooth muscle cell markers. As shown in Figure 5, the immunoreactivity of HK-2 significantly increased in the lung tissue of MCT rats, and the positive signals were predominantly found in the perivascular area, while 3-BrPA reversed this effect.

Aerobic glycolysis results from increased glucose uptake, glucose transporter protein-1 (GLUT1) plays a critical role

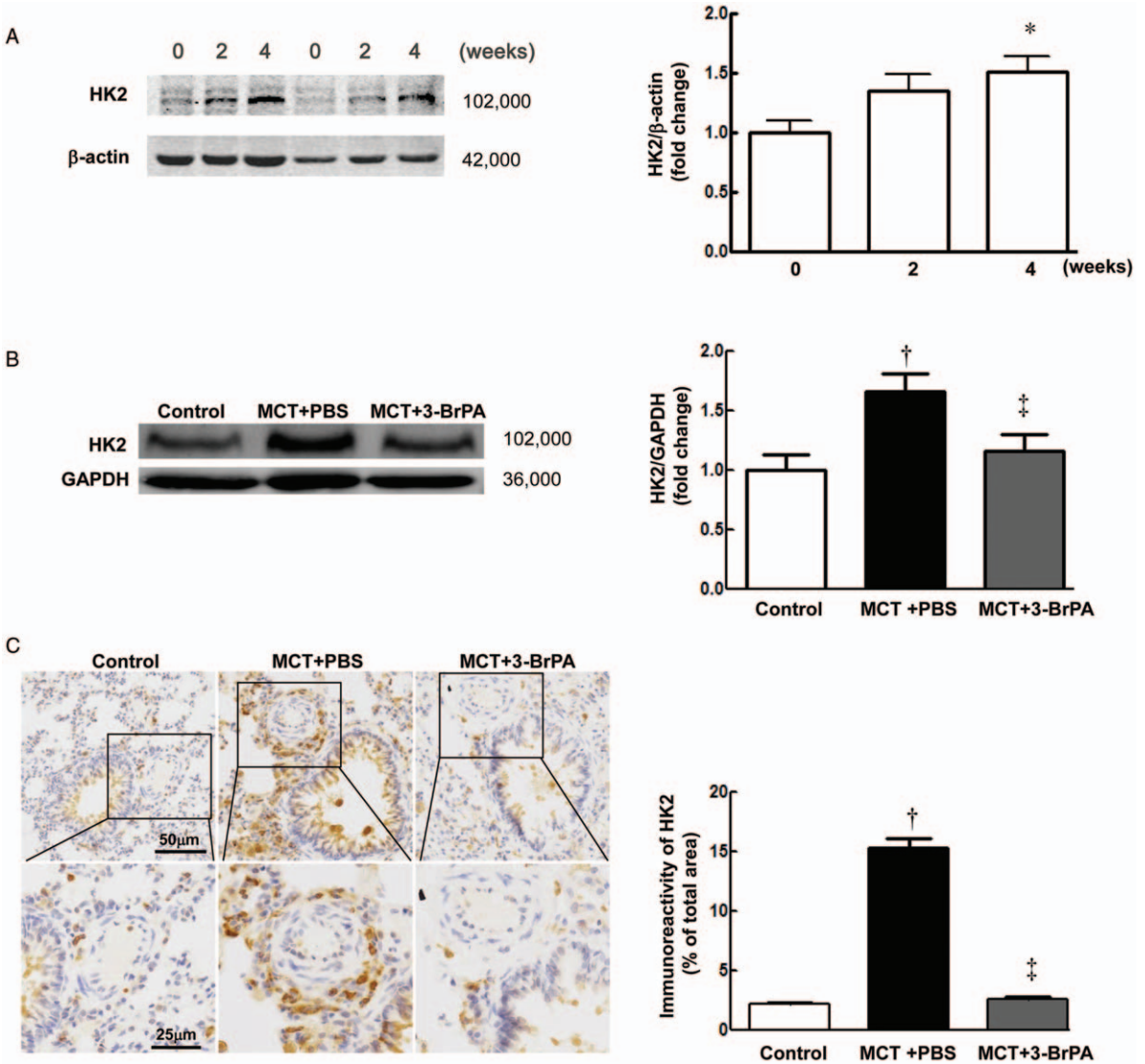

Figure 4: Expression level of HK-2 in MCT rats and the effect of 3-BrPA on HK-2 expression. (A) The protein level of HK-2 was determined by Western blotting at 2 and 4 weeks after MCT injection and was normalized to the expression of β-actin ($^{*}P < 0.05$ *vs.* baseline, $n = 6$ in each group). (B) The protein level of HK-2 was determined by Western blotting ($n = 5$ in each group) in control, MCT + PBS-treated, and MCT + 3-BrPA-treated groups ($^{\dagger}P < 0.05$ *vs.* control; $^{\ddagger}P < 0.05$ *vs.* MCT + PBS). (C) The protein level of HK-2 was determined by immunochemistry ($n = 3$ in each group) in control, MCT + PBS-treated, and MCT + 3-BrPA-treated groups ($^{\dagger}P < 0.001$ *vs.* control; $^{\ddagger}P < 0.001$ *vs.* MCT + PBS). Upper panel: Scale bar = 50 μm; lower panel: Scale bar = 25 μm. 3-BrPA: 3-Bromopyruvate; GAPDH: Glyceraldehyde-3-phosphate dehydrogenase; HK-2: Hexokinase 2; MCT: Monocrotaline; PBS: Phosphate-buffered saline.

in glucose uptake, and increased expression of GLUTs is responsible for aerobic glycolysis. As shown in Figure 6, MCT induced the expression of GLUT1, while 3-BrPA reversed this effect.

Effects of 3-BrPA on apoptosis

Several lines of evidence suggest that 3-BrPA induces apoptosis in cancer cells.[13,14] The effects of 3-BrPA on apoptosis in MCT rats were further examined by measuring the changes in the expression of apoptosis-associated proteins. The amount of cleaved Casp 3 protein expression was increased in the 3-BrPA treatment MCT rats [Figure 7A]. Furthermore, we observed decreased Cyto C in mitochondria [Figure 7B] and increased the release of Cyto C into the cytoplasm in the 3-BrPA-treated MCT rats compared to those of PBS-treated MCT rats [Figure 7C]. These results show that 3-BrPA leads to the activation of the mitochondrial apoptotic signaling pathway.

A TUNEL assay was used to further investigate the apoptosis effect of 3-BrPA, as shown in Figure 7D. TUNEL-positive cells in the lung tissue of 3-BrPA-treated MCT rats were significantly increased compared with those of control and PBS-treated MCT rats.

Effects of 3-BrPA on inflammatory infiltration

Inflammatory infiltration and macrophage invasion have been shown to represent key features in PH.[15] We thus evaluated the macrophage content in the lungs of all three animal groups [Figure 8]. The number of macrophages and CD68-positive cells in the lungs of PBS-treated MCT rats was significantly higher than that in the control group. In

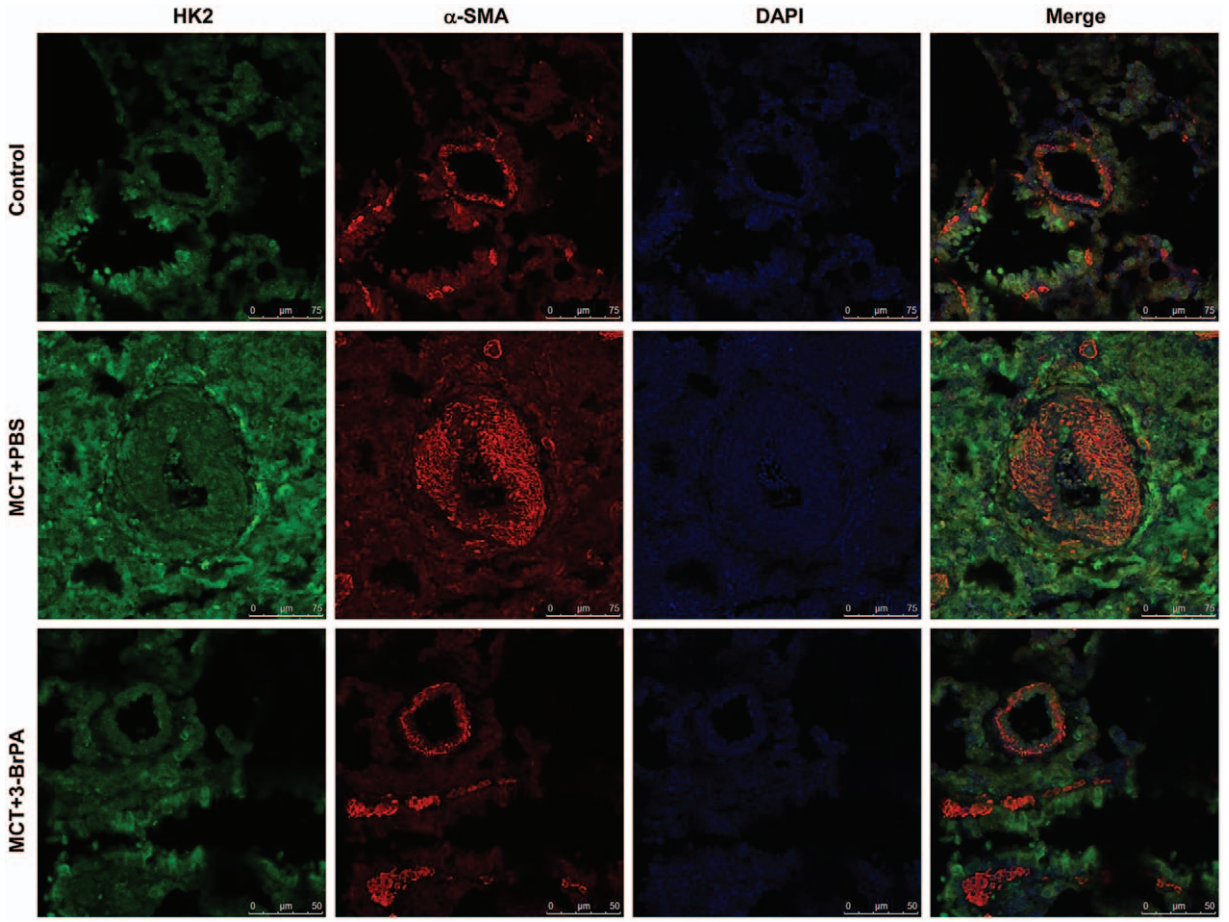

Figure 5: Co-staining of smooth muscle actin and HK-2. Immunofluorescent staining of smooth muscle actin (red) and HK-2 (green) in representative histological sections from paraffin-embedded lung tissues of control, MCT + PBS-treated, and MCT + 3-BrPA-treated groups. Nuclei were labeled by DAPI (blue). Scale bar = 75 μm. 3-BrPA: 3-Bromopyruvate; α-SMA: α-Smooth muscle actin; DAPI: 4′,6-Diamidino-2-phenylindole; HK-2: Hexokinase 2; MCT: Monocrotaline; PBS: Phosphate-buffered saline.

contrast, 3-BrPA treatment of MCT rats showed a reduction compared to that of PBS-treated MCT rats. Thus, in addition to beneficial hemodynamic and structural changes in the lung and heart by 3-BrPA, inflammatory infiltration was also effectively reduced. To investigate the localization of macrophages in the lung tissue, co-staining of CD68 and smooth muscle cell markers was performed and showed that MCT-induced macrophage infiltration was mainly located in the perivascular area [Figure 9] and that 3-BrPA reversed MCT-induced macrophage infiltration.

Discussion

In this study, we demonstrated a significantly increased rate of aerobic glycolysis in the MCT-induced PH rats. Treatment with 3-BrPA, a glycolysis inhibitor, was effective in reducing right ventricular systolic pressure, pulmonary arteriolar remodeling, and right ventricular hypertrophy via inhibiting HK-2, activating the apoptosis pathway and suppressing PH-associated lung inflammation, indicating that 3-BrPA has the potential to be an attractive therapeutic strategy in treating PH.

PH represents a fatal disease with limited therapeutic options targeting the nitric oxide, prostacyclin, and endothelin pathways, and the current life expectancy is comparable to that of metastatic cancer.[16] In recent decades, many researchers have found that PH and cancer share similar poor prognoses and major pathophysiological mechanisms, including increased cell proliferation, apoptosis resistance, and metabolic shift.[17] Interestingly, studies have reported that the tissue of PH patients and experimental PH exhibit the Warburg effect, which indicates that the pathogenesis of PH is similar to that of cancer biology.[18]

Lactate production and glucose consumption, typical features of the Warburg effect, and HK-2, the essential enzyme for aerobic glycolysis, were reported to be increased in pulmonary arterial smooth muscle cells of chronic thromboembolic pulmonary hypertension patients.[3] Consistent with our previous findings, the present study showed that lactate production, glucose consumption, and expression of HK-2 were also increased in MCT rats.

HKs catalyzes the first irreversible step in glycolysis. There are four major isoforms (HK-1, HK-2, HK-3, and HK-4)

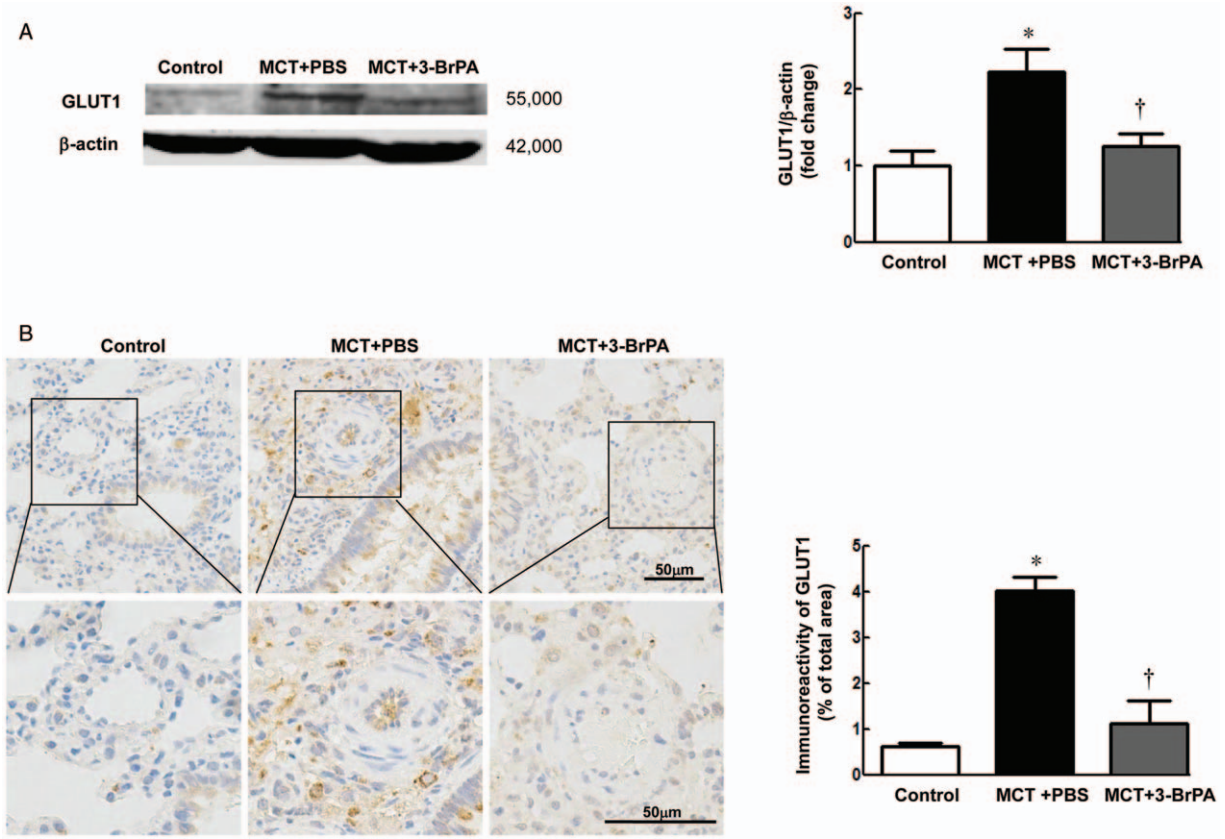

Figure 6: Expression level of GLUT1 and the effect of 3-BrPA on GLUT1 expression. (A) Protein levels of GLUT1 were determined by Western blotting ($n = 6$ in each group) in control, MCT + PBS-treated, and MCT + 3-BrPA-treated groups ($^{*}P < 0.01$ *vs.* control; $^{\dagger}P < 0.05$ *vs.* MCT + PBS). (B) Protein levels of GLUT1 were determined by immunochemistry ($n = 3$ in each group) in control, MCT + PBS-treated, and MCT + 3-BrPA-treated groups ($^{*}P < 0.001$ *vs.* control; $^{\dagger}P < 0.001$ *vs.* MCT + PBS). Upper panel: Scale bar = 50 μm; lower panel: Scale bar = 25 μm. 3-BrPA: 3-Bromopyruvate; GLUT1: Glucose transporter protein-1; MCT: Monocrotaline; PBS: Phosphate-buffered saline.

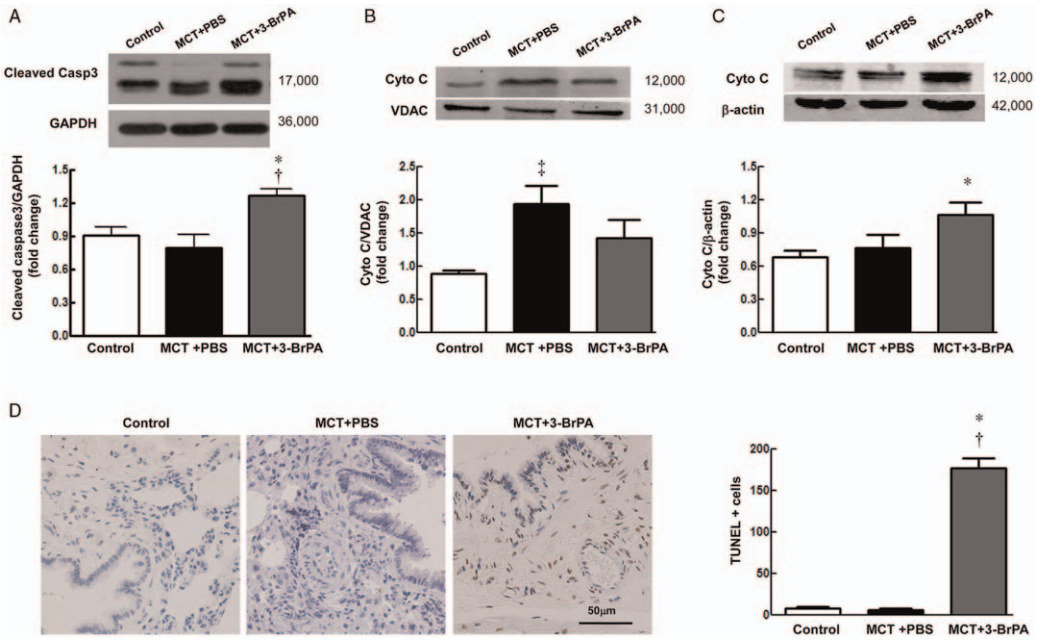

Figure 7: Effects of 3-BrPA on apoptosis in MCT-induced PH rats. (A) Expression levels of cleaved Casp 3 ($n = 5$ in each group) in lung tissues, (B) Cyto C in mitochondria ($n = 6$ in each group), and (C) Cyto C in cytoplasm ($n = 6$ in each group) were analyzed by Western blotting analysis of lung tissue samples from control, MCT + PBS, and MCT + 3-BrPA groups. The level of each protein was calculated after normalizing its intensity to that of GAPDH, VDAC, or β-actin. Values obtained were plotted as histograms ($^{*,\ddagger}P < 0.05$ *vs.* control, $^{\dagger}P < 0.05$ *vs.* MCT + PBS). (D) TUNEL assays showing apoptotic cells in lung tissues from control, MCT + PBS, and MCT+3-BrPA groups. The brown cells represent the apoptotic cells determined by TUNEL assay. The calculated TUNEL-positive cells were plotted as histograms ($^{*}P < 0.001$ *vs.* control, $^{\dagger}P < 0.001$ *vs.* MCT + PBS). 3-BrPA: 3-Bromopyruvate; Casp 3: Caspase-3; Cyto C: Cytochrome C; GAPDH: Glyceraldehyde-3-phosphate dehydrogenase; MCT: Monocrotaline; PBS: Phosphate-buffered saline; TUNEL: Terminal deoxynucleotidyl transferase-mediated dUTP-biotin nick end-labeling; VDAC: Voltage-dependent anion channel.

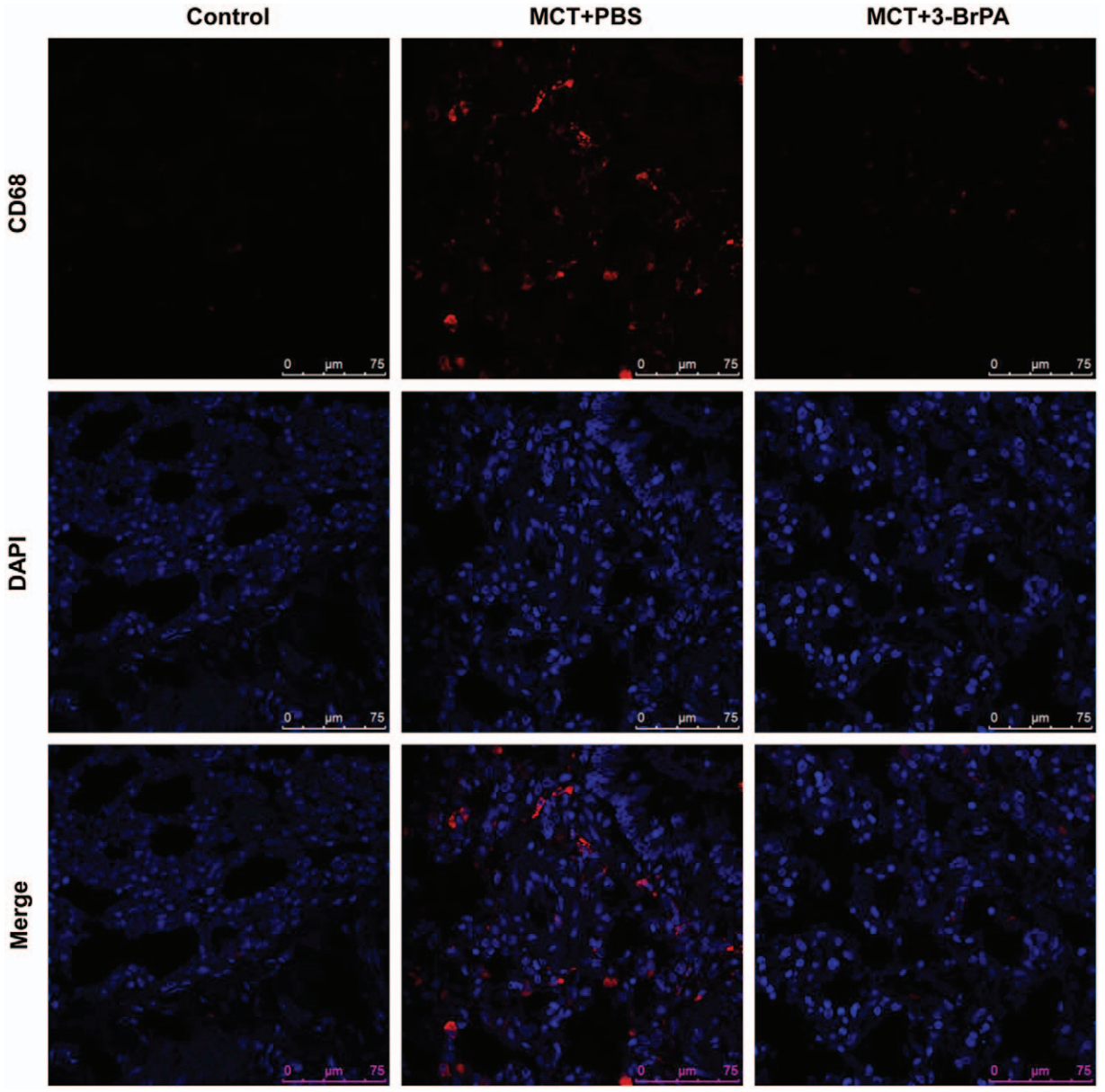

Figure 8: Effects of 3-BrPA on lung inflammation in MCT rats. Representative lung immunofluorescence staining with an antibody against the macrophage marker CD68 for the detection of macrophages in control, MCT + PBS-treated, and MCT + 3-BrPA-treated groups. Scale bar = 75 μm. 3-BrPA: 3-Bromopyruvate; DAPI: 4′,6-Diamidino-2-phenylindole; MCT: Monocrotaline; PBS: Phosphate-buffered saline.

characterized in mammalian tissue.[19] Among these different HKs, HK-2 is often overexpressed in many tumors. The upregulated HK-2 binds to the mitochondrial VDACs and promotes tumor cell proliferation and survival by inhibiting Cyto C release and escaping from apoptosis.[20] These results suggest that HK-2 has a potential role in the development of PH. However, the mechanism was not identified in our study. Hypoxia-inducible factor-1α (HIF-1α) activation plays an important role in cellular metabolism.[6] In addition, the proximal promoter of HK-2 contains binding sites for HIF-1α.[21] Therefore, we hypothesize that HIF-1α transcriptionally upregulates glycolysis via increased expression of HK-2 in MCT rats.

3-BrPA has been described recently as a remarkably effective anti-cancer drug by rapidly inhibiting tumor cell growth in tissue culture, eradicating cancers in animals, and preventing metastasis.[7] It has been reported that 3-BrPA inhibits the energy-obtaining process of tumor cells by inhibiting the activities of metabolic enzymes[8,9] and regulating the expression of substance transport carriers and signaling pathways involved in cell division, autophagy, and apoptosis.[22,23] Among these, 3-BrPA is also used as a typical inhibitor of HK-2 via alkylation.[10,23,24] In this study, we showed that treatment with 3-BrPA was effective in reducing aerobic glycolysis, right ventricular systolic pressure, pulmonary arteriolar remodeling, and right ventricular hypertrophy in MCT rats. A previous study demonstrated that 3-BrPA inhibited glycolysis as well as mitochondria-bound HK-2 and consequently led to apoptosis in cancer cells.[25] In the current study, we demonstrated that 3-BrPA downregulated the expression

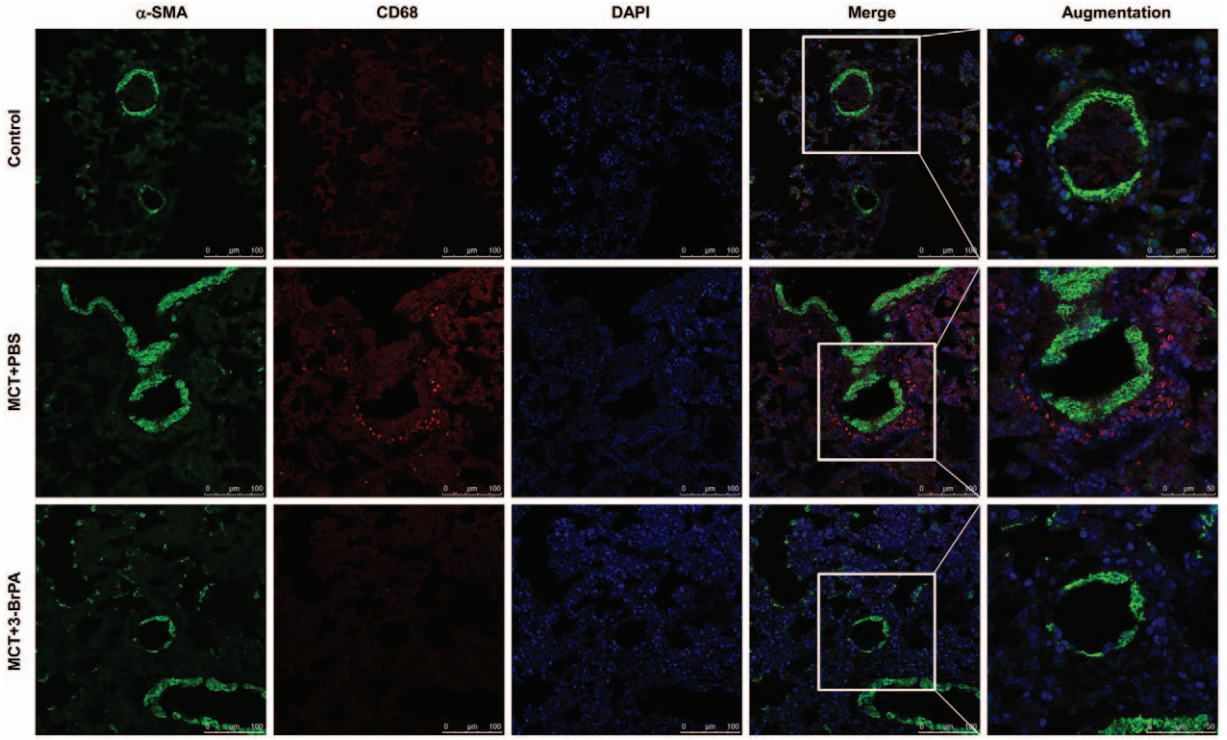

Figure 9: Co-staining of smooth muscle actin and CD68. Immunofluorescent staining of smooth muscle actin (green) and CD68 (red) in representative histological sections from paraffin-embedded lung tissues from control, MCT + PBS-treated, and MCT + 3-BrPA-treated groups. Nuclei were labeled by DAPI (blue). Scale bar = 50 μm for augmentation pictures and 100 μm for the remaining pictures. 3-BrPA: 3-Bromopyruvate; α-SMA: α-Smooth muscle actin; DAPI: 4′,6-Diamidino-2-phenylindole; MCT: Monocrotaline; PBS: phosphate-buffered saline.

of HK-2 and promoted apoptosis in MCT-PH rats through increased release of proapoptotic mediators such as Cyto C and cleaved Casp 3. Therefore, these data suggest that 3-BrPA is effective against MCT-PH via downregulating HK-2 and activating mitochondrial apoptosis.

PH is characterized by increased production of proinflammatory cytokines and perivascular inflammatory features.[26] Finally, we evaluated the potential influence of 3-BrPA on pulmonary inflammation by determining the abundance of macrophages in the lung. MCT rats were associated with a highly elevated content of cells that were positive for the macrophage biomarker CD68, and when MCT rats were treated with 3-BrPA, the number of CD68-positive cells was reduced. Thus, 3-BrPA also effectively reduced inflammatory infiltration in MCT rats.

Our results provide evidence that 3-BrPA, a glycolysis inhibitor, is effective in reducing multiple pathological processes in MCT-induced PH, including aerobic glycolysis, right ventricular systolic pressure, pulmonary arteriolar remodeling, and right ventricular hypertrophy. These data also demonstrate that 3-BrPA exerts its beneficial effect on PH by targeting HK-2 in a manner that was associated with inducing apoptosis and suppressing inflammation. In conclusion, our findings suggest that 3-BrPA might has a potential beneficial effect on the PH treatment.

Funding

This work was supported by grants from the National Natural Science Foundation of China (No. 31600939), the Beijing Natural Science Foundation (No. 7174280), and the Beijing Talents Training Project (No. 2015000020124G111).

Conflicts of interest

None.

References

1. Ataya A, Cope J, Alnuaimat H. A review of targeted pulmonary arterial hypertension-specific pharmacotherapy. J Clin Med 2016;5:114. doi: 10.3390/jcm5120114.
2. Benza RL, Miller DP, Barst RJ, Badesch DB, Frost AE, McGoon MD. An evaluation of long-term survival from time of diagnosis in pulmonary arterial hypertension from the REVEAL registry. Chest 2012;142:448–456. doi: 10.1378/chest.11-1460.
3. Wang L, Gan HL, Liu Y, Gu S, Li J, Guo LJ, *et al*. The distinguishing cellular features of pulmonary artery smooth muscle cells from chronic thromboembolic pulmonary hypertension patients. Exp Lung Res 2013;39:349–358. doi: 10.3109/01902148.2013.822947.
4. Harvey LD, Chan SY. Emerging metabolic therapies in pulmonary arterial hypertension. J Clin Med 2017;6:43. doi: 10.3390/jcm6040043.
5. Vander Heiden MG, Cantley LC, Thompson CB. Understanding the Warburg effect: the metabolic requirements of cell proliferation. Science 2009;324:1029–1033. doi: 10.1126/science.1160809.
6. Tuder RM, Davis LA, Graham BB. Targeting energetic metabolism: a new frontier in the pathogenesis and treatment of pulmonary hypertension. Am J Respir Crit Care Med 2012;185:260–266. doi: 10.1164/rccm.201108-1536PP.
7. Lis P, Dylag M, Niedzwiecka K, Ko YH, Pedersen PL, Goffeau A, *et al*. The HK2 dependent "Warburg effect" and mitochondrial oxidative phosphorylation in cancer: targets for effective therapy with 3-bromopyruvate. Molecules 2016;21:1730. doi: 10.3390/molecules21121730.

8. Shoshan MC. 3-Bromopyruvate: targets and outcomes. J Bioenerg Biomembr 2012;44:7–15. doi: 10.1007/s10863-012-9419-2.
9. Ganapathy-Kanniappan S, Geschwind JF, Kunjithapatham R, Buijs M, Vossen JA, Tchernyshyov I, *et al*. Glyceraldehyde-3-phosphate dehydrogenase (GAPDH) is pyruvylated during 3-bromopyruvate mediated cancer cell death. Anticancer Res 2009;29:4909–4918.
10. Gao S, Chen X, Jin H, Ren S, Liu Z, Fang X, *et al*. Overexpression of ErbB2 renders breast cancer cells susceptible to 3-BrPA through the increased dissociation of hexokinase II from mitochondrial outer membrane. Oncol Lett 2016;11:1567–1573. doi: 10.3892/ol.2015.4043.
11. Chen F, Wang H, Lai J, Cai S, Yuan L. 3-Bromopyruvate reverses hypoxia-induced pulmonary arterial hypertension through inhibiting glycolysis: in vitro and in vivo studies. Int J Cardiol 2018;266:236–241. doi: 10.1016/j.ijcard.2018.03.104.
12. Kunjithapatham R, Geschwind JF, Rao PP, Boronina TN, Cole RN, Ganapathy-Kanniappan S. Systemic administration of 3-bromopyruvate reveals its interaction with serum proteins in a rat model. BMC Res Notes 2013;6:277. doi: 10.1186/1756-0500-6-277.
13. Wang TA, Zhang XD, Guo XY, Xian SL, Lu YF. 3-bromopyruvate and sodium citrate target glycolysis, suppress survivin, and induce mitochondrial-mediated apoptosis in gastric cancer cells and inhibit gastric orthotopic transplantation tumor growth. Oncol Rep 2016;35:1287–1296. doi: 10.3892/or.2015.4511.
14. Ganapathy-Kanniappan S, Geschwind JF, Kunjithapatham R, Buijs M, Syed LH, Rao PP, *et al*. 3-Bromopyruvate induces endoplasmic reticulum stress, overcomes autophagy and causes apoptosis in human HCC cell lines. Anticancer Res 2010;30:923–935. doi:10.1097/CAD.0b013e32833418c0.
15. Kumar R, Graham B. How does inflammation contribute to pulmonary hypertension? Eur Respir J 2018;51:1702403. doi: 10.1183/13993003.02403-2017.
16. Michelakis ED. Pulmonary arterial hypertension: yesterday, today, tomorrow. Circ Res 2014;115:109–114. doi: 10.1161/CIRCRESAHA.115.301132.
17. Archer SL. Pyruvate kinase and Warburg metabolism in pulmonary arterial hypertension: uncoupled glycolysis and the cancer-like phenotype of pulmonary arterial hypertension. Circulation 2017;136:2486–2490. doi: 10.1161/CIRCULATIONAHA.117.031655.
18. Boucherat O, Vitry G, Trinh I, Paulin R, Provencher S, Bonnet S. The cancer theory of pulmonary arterial hypertension. Pulm Circ 2017;7:285–299. doi: 10.1177/2045893217701438.
19. Wilson JE. Isozymes of mammalian hexokinase: structure, subcellular localization and metabolic function. J Exp Biol 2003;206:2049–2057. doi: 10.1242/jeb. 00241.
20. Mathupala SP, Ko YH, Pedersen PL. Hexokinase II: cancer's double-edged sword acting as both facilitator and gatekeeper of malignancy when bound to mitochondria. Oncogene 2006;25:4777–4786. doi: 10.1038/sj.onc.1209603.
21. Botzer LE, Maman S, Sagi-Assif O, Meshel T, Nevo I, Yron I, *et al*. Hexokinase 2 is a determinant of neuroblastoma metastasis. Br J Cancer 2016;114:759–766. doi: 10.1038/bjc.2016.26.
22. Birsoy K, Wang T, Possemato R, Yilmaz OH, Koch CE, Chen WW, *et al*. MCT1-mediated transport of a toxic molecule is an effective strategy for targeting glycolytic tumors. Nat Genet 2013;45:104–108. doi: 10.1038/ng.2471.
23. Zhang Q, Zhang Y, Zhang P, Chao Z, Xia F, Jiang C, *et al*. Hexokinase II inhibitor, 3-BrPA induced autophagy by stimulating ROS formation in human breast cancer cells. Genes Cancer 2014;5:100–112. doi: 10.18632/genesandcancer.9.
24. Xian SL, Cao W, Zhang XD, Lu YF. 3-Bromopyruvate inhibits human gastric cancer tumor growth in nude mice via the inhibition of glycolysis. Oncol Lett 2016;12:5377. doi: 10.3892/ol.2016.5370.
25. Sun Y, Liu Z, Zou X, Lan Y, Sun X, Wang X, *et al*. Mechanisms underlying 3-bromopyruvate-induced cell death in colon cancer. J Bioenerg Biomembr 2015;47:319–329. doi: 10.1007/s10863-015-9612-1.
26. Florentin J, Dutta P. Origin and production of inflammatory perivascular macrophages in pulmonary hypertension. Cytokine 2017;100:11–15. doi: 10.1016/j.cyto.2017.08.015.

How to cite this article: Liu J, Wang W, Wang L, Qi XM, Sha YH, Yang T. 3-Bromopyruvate alleviates the development of monocrotaline-induced rat pulmonary arterial hypertension by decreasing aerobic glycolysis, inducing apoptosis, and suppressing inflammation. Chin Med J 2020;133:49–60. doi: 10.1097/CM9.0000000000000577